

THERMAL DECOMPOSITION AND MELTING OF A NEW CARBOXYINDOLE DERIVATIVE

A. Marini¹, V. Berbenni¹, G. Bruni¹, M. Villa² and A. Orlandi³

¹C.S.G.I. e CSTE-CNR - Dipartimento di Chimica Fisica dell'Università di Pavia, Viale Taramelli 16, 27100 Pavia, Italy

²Dipartimento di Ingegneria dell'Università di Bergamo e Unità INFM of Pavia, Italy

³GlaxoWellcome, Medicines Research Center, Via A. Fleming 2, 37135 Verona, Italy

Abstract

GV150526A is a novel 2-carboxyindole derivative, recently synthesized by GlaxoWellcome, which is used in treatment or prevention of CNS disorders resulting from neurotoxic damage.

It has been prepared in three forms, F1, F2 and F3, having significantly different hydration/dehydration behavior and/or diffraction patterns. Here, we extend the thermal analysis of these polymorphs above 200°C, where all forms are fully dehydrated and the main thermal phenomena are decomposition and melting. Simultaneous TG/DSC measurements have been repeated in wet and dry nitrogen atmospheres over a wide range of heating rates. Form F3 displays a qualitatively different behavior relative to F1 and F2. This fact is interpreted as an evidence of a mechanism of decomposition which sets F3 apart from F1 and F2. The thermal data are summarized by simple heuristic equations and few 'apparent' enthalpies.

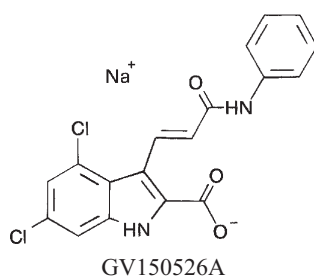
Keywords: melting, simultaneous TG/DSC, thermal decomposition

Introduction

GlaxoWellcome has recently developed a new class of drugs useful in the treatment or prevention of CNS disorders resulting from neurotoxic damage, such as cerebral ischemia or thromboembolic stroke, and from chronic neurodegenerative diseases, such as Alzheimer's senile dementia, epilepsy, depression, and drug dependency. These drugs are novel 2-carboxyindole derivatives which are effective antagonist of the NMDA receptor complex [1]. One of the most promising compounds of this class has been named GV150526A: it is a sodium salt of (E)-3-[2-(phenylcarbamoyl)-ethenyl]-4,6, dichloroindole-2-carboxylic acid.

It has a strong and selective action at the strychnine insensitive glycine binding site, which is coupled with an excellent bioavailability. GV150526A has been prepared in three crystal forms (F1, F2, F3) with the same water content (1.5 mol/compound mol), thus representing a case of polymorphism of a pseudopolymorph. A careful analysis of their dehydration/rehydration properties has shown that thermal methods are better suited than X-ray diffraction, liquid chromatography and optical

spectroscopy in discriminating among different polymorphs and, in particular, between the nearly identical forms F1 and F2 [2]. With thermal methods, we may even reliably estimate the fraction of each polymorph in a mixture [2]. Furthermore, we found that F1 and F3 convert to F2 (the form thermodynamically stable at room temperature) upon cooling after heating to 120°C. In this paper, the thermal investigation is extended above 200°C where all forms are fully dehydrated but still display significantly different thermal behaviors. We will begin by commenting the major trends displayed by the data; these trends will be interpreted in the framework of ‘zero order’ heuristic models, with no other pretense than summarizing the main features of the complex phenomena involved with decomposition and melting of GV150526A.



Experimental

GV150526A samples come from batches of industrial production controlled by HPLC. Their thermal stability was characterized with simultaneous TG/DSC measurements performed with the STA 625 system of Polymer Laboratories (UK). The measurements covered the 20–370°C range and were performed either in a flow (35 mL min⁻¹) of dry nitrogen, or a flow of nitrogen bubbled through water at room temperature (wet nitrogen). The heating rates (β) ranged from 1 to 30 K min⁻¹. Typical traces obtained with the lowest (1 K min⁻¹) and with the highest (30 K min⁻¹) scanning rate are presented in Fig. 1. The endothermic DSC peaks of the two traces are quite different, and are completed well before the sample mass becomes constant. As it will be discussed below, this thermal phenomenon is due to decomposition and melting.

Quantitative data have been extracted from these traces as follows: the decomposition/melting enthalpy (ΔH_{exp}) is computed relative to a baseline which extrapolates the DSC trace before the peak, up to where the trace moving in the exothermic direction crosses this baseline. To the DSC peak we associate the fractional mass loss ($\Delta m\%$ – referred to the sample mass at room temperature) which occurs under the peak, i.e. between the two temperatures (T_c and T_p) identified by crosses in Fig. 1. Typically, temperatures are reproduced within 1°C, enthalpies within 5% and mass losses within 3%. To the difference of our previous work [2], where the point was to use small but significant variations of mass loss for diagnostic purposes, here we are interested mainly in the qualitative differences among samples. For this reason, the data will be rounded to the least significant digit and shown with no other indication

of error. To show the reproducibility of our data, in the tables we occasionally quote repeated measurements at the same β .

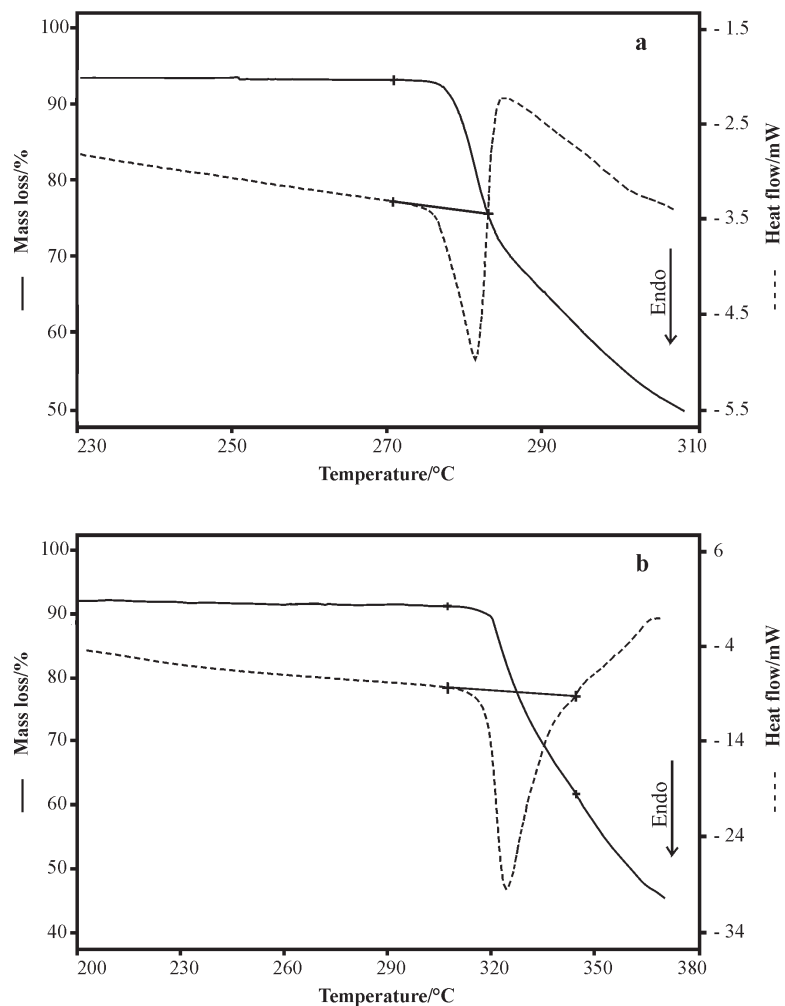


Fig. 1 Simultaneous TG/DSC traces obtained with form F2 at different heating rates; the peak area is computed between the two crosses (at T_e and T_f) as explained in the text: a – $\beta=1 \text{ K min}^{-1}$; b – $\beta=30 \text{ K min}^{-1}$

Results

Onset temperatures

We will begin by discussing the onset temperatures, which are reported in Tables 1–3 for polymorphs F1, F2 and F3, respectively. These onset temperatures (T_o) increase

by $\sim 40^\circ\text{C}$ in going from the lowest to the highest scanning rate*. The overall shift of T_e is nearly the same for forms F1 and F2, and substantially smaller for form F3. Furthermore, in forms F1 and F2 the onset temperatures at the same β are systematically higher (by several degrees) in wet nitrogen than in dry nitrogen while, in form F3, these temperatures are not affected by the presence of water vapor.

Both the strong dependence of T_e upon β and a loss of mass concurrent with the DSC peak suggest that decomposition is involved in this thermal phenomenon. Since F3 has onset temperatures significantly lower than F1 and F2, it is confirmed [2] that F3 is the least stable form. A more important difference is that T_e in the dehydrated F3 form is apparently not affected by the presence of water vapor (as it is the case for F1 and F2), a fact which is believed to be related with the different hydration behavior of F3 relative to F1 and F2 [2].

Mass changes

The mass losses ($\Delta m\%$, Tables 1–3) always increase with increasing β . Such a dependence upon the heating rate is apparently unusual for a decomposition, since a smaller β means a longer time spent in the temperature region of the peak, and therefore a better chance to complete a kinetic reaction yielding gaseous products. From Fig. 1, we note that the DSC peak is somehow broader at higher β ; as a consequence, the time needed to scan through the peak region, t_{peak} , does not scale exactly as $1/\beta$. However, t_{peak} decreases by a factor of ten in going from 1 to 30 K min^{-1} .

Table 1 Extrapolated onset temperatures (T_e), final temperatures (T_f), mass losses (Δm) and peak enthalpies (ΔH_{exp}) of F1 under dry nitrogen (a) and wet nitrogen (b)

| | $\beta/\text{K min}^{-1}$ | $T_e/^\circ\text{C}$ | $T_f/^\circ\text{C}$ | $\Delta m/\%$ | $\Delta H_{\text{exp}}/\text{J g}^{-1} \text{ sample}$ |
|---|---------------------------|----------------------|----------------------|---------------|--|
| a | 30 | 320 | 345 | 30 | 148 |
| | 20 | 315 | 336 | 28 | 139 |
| | 10 | 304 | 321 | 26 | 141 |
| | 5 | 296 | 305 | 19 | 122 |
| | 1 | 276 | 282 | 16 | 117 |
| b | 30 | 323 | 350 | 36 | 154 |
| | 10 | 310 | 329 | 34 | 148 |
| | 2 | 290 | 297 | 22 | 128 |
| | 1 | 281 | 287 | 19 | 114 |
| | 1 | 282 | 288 | 22 | 119 |

* Note that a typical melting phenomenon is expected to be almost independent from β . As a matter of fact, with our apparatus, the onset temperature for the melting of indium increases of about 0.27°C when the rate is changed from 0.2 to $30^\circ\text{C min}^{-1}$.

Table 2 Extrapolated onset temperatures (T_e), final temperatures (T_f), mass losses (Δm) and peak enthalpies (ΔH_{exp}) of F2 under dry nitrogen (a) and wet nitrogen (b)

| | $\beta/\text{K min}^{-1}$ | $T_e/^\circ\text{C}$ | $T_f/^\circ\text{C}$ | $\Delta m/\%$ | $\Delta H_{\text{exp}}/\text{J g}^{-1}\text{ sample}$ |
|---|---------------------------|----------------------|----------------------|---------------|---|
| a | 30 | 319 | 344 | 30 | 148 |
| | 20 | 314 | 336 | 30 | 152 |
| | 10 | 305 | 315 | 20 | 122 |
| | 10 | 305 | 321 | 23 | 130 |
| | 1 | 276 | 283 | 17 | 120 |
| b | 30 | 322 | 349 | 33 | 149 |
| | 20 | 317 | 340 | 32 | 141 |
| | 10 | 308 | 324 | 28 | 131 |
| | 5 | 300 | 314 | 27 | 121 |
| | 1 | 280 | 286 | 18 | 108 |

Table 3 Extrapolated onset temperatures (T_e), final temperatures (T_f), mass losses (Δm) and peak enthalpies (ΔH_{exp}) of F3 under dry nitrogen (a) and wet nitrogen (b)

| | $\beta/\text{K min}^{-1}$ | $T_e/^\circ\text{C}$ | $T_f/^\circ\text{C}$ | $\Delta m/\%$ | $\Delta H_{\text{exp}}/\text{J g}^{-1}\text{ sample}$ |
|---|---------------------------|----------------------|----------------------|---------------|---|
| a | 30 | 312 | 346 | 30 | 153 |
| | 20 | 306 | 335 | 28 | 155 |
| | 10 | 300 | 321 | 26 | 159 |
| | 5 | 293 | 311 | 26 | 152 |
| | 1 | 276 | 286 | 21 | 154 |
| b | 30 | 312 | 344 | 30 | 148 |
| | 30 | 312 | 345 | 31 | 146 |
| | 10 | 300 | 322 | 28 | 133 |
| | 5 | 293 | 313 | 27 | 131 |
| | 2 | 278 | 286 | 22 | 117 |

From Fig. 1 and Tables 1–3, it is apparent that a major effect of a faster scan is to increase the closing temperature of the peak, T_f , which changes more with β than T_e does. Since the process of mass loss always begins after T_e and is still underway at T_f , it is expected that the mass loss increases with T_f , even if the effect is somehow mitigated by the overall shift to high temperatures, with increasing β , of the mass loss trace. Regression analysis of the $\Delta m\%$ vs. T_f data yields correlation coefficients ranging from 0.92 and 0.99, with slopes going from ~ 0.15 (for F3) to $\sim 0.3\%/^\circ\text{C}$ (for F1 and F2). These slopes have little or no dependence upon the atmosphere. On the other hand, the changes of mass are systematically higher in wet nitrogen than in dry nitrogen (~ 1 in F3, and $\sim 4\%$ in F1 and F2).

Decomposition/melting enthalpies

Tables 1–3 show that peak enthalpies are systematically higher in dry nitrogen. It is as if some sort of reaction occurred with water vapor which favors decomposition or melting. With the exception of F3 in dry nitrogen, where peak enthalpies are independent of β , ΔH_{exp} increases with the heating rate, or with $\Delta m\%$. We call attention to this major qualitative difference, which definitely sets F3 apart from the other forms.

Discussion

The phenomena presented above indicate that neither simple decomposition (with an enthalpy proportional to the mass loss) nor simple melting (with a rate-independent onset temperature) occur in our samples. Furthermore, the substantial differences between form F1 & F2 on one hand, and form F3 on the other, suggest separate treatments.

A model for decomposition and melting of F1 and F2 forms

We assume that, in both dry and wet nitrogen, melting follows decomposition and that the fractions of the sample which may ‘decompose’, m_d/m_i (m_i is the initial sample mass at room temperature), and which actually ‘melts’, m_{fus}/m_i , depend upon the experimental conditions. We assign average enthalpies per unit mass, ΔH_d and ΔH_{fus} , to decomposition and melting and assume that the observed enthalpy, ΔH_{exp} (referred to $m_i=1$ g), is a weighed sum of ΔH_d and ΔH_{fus}

$$\Delta H_{\text{exp}} = \Delta H_{\text{fus}} \frac{m_{\text{fus}}}{m_i} + \Delta H_d \frac{m_d}{m_i} \quad (1)$$

We have no direct access to m_d , but it is reasonable to say that it is proportional to the loss of mass taking place during the endothermic peak. Here, we will identify m_d with the experimental change of mass, $\Delta m\%$, as it would be the case where decomposition involves only gaseous products. Therefore we set

$$\frac{m_d}{m_i} = \frac{|\Delta m\%|}{100} \quad (2)$$

To estimate m_{fus} , we assume that melting has involved the entire mass of the sample remaining at T_r . We recall that the thermal phenomena under study occur after the samples have lost about 6.5% of the original mass during dehydration ($\Delta m_{\text{H}_2\text{O}}$) [2]; note in Fig. 1 that the mass loss around 200°C is about 93% of the mass at the beginning of the run. Therefore we write

$$\frac{m_{\text{fus}}}{m_i} = \frac{100 - |\Delta m_{\text{H}_2\text{O}}| - |\Delta m\%|}{100} \quad (3)$$

By combining the above equations we have

$$\Delta H_{\text{exp}} = \Delta H_{\text{fus}} \frac{100 - |\Delta m_{\text{H}_2\text{O}}|}{100} + \frac{|\Delta m\%|}{100} (\Delta H_{\text{d}} - \Delta H_{\text{fus}}) \quad (4)$$

This equation predicts a linear relationship between ΔH_{exp} and $\Delta m\%$, as it should be since Tables 1–3 show that these quantities are both linearly related to T_r . Therefore, with a linear regression analysis of the ΔH_{exp} vs. $\Delta m\%$ data we may retrieve what will be called the ‘apparent enthalpies’ ΔH_{d} and ΔH_{fus} for samples F1 and F2 in dry and wet atmospheres (Table 4). Of course, we should not attach a precise meaning to these apparent enthalpies, since we really ignore how much of the sample actually ‘decomposes’ and how much ‘melts’. However, a discussion of ΔH_{d} and ΔH_{fus} in relative terms is certainly meaningful.

Table 4 Apparent melting and decomposition enthalpies (ΔH_{fus} , ΔH_{d}) for forms F1 and F2 in dry nitrogen (a) and wet nitrogen (b)

| | | $\Delta H_{\text{fus}}/\text{J g}^{-1}$ | $\Delta H_{\text{d}}/\text{J g}^{-1}$ |
|----|---|---|---------------------------------------|
| F1 | a | 86 | 306 |
| | b | 80 | 296 |
| F2 | c | 79 | 333 |
| | d | 63 | 322 |

According to Eq. (4), the more of the sample decomposes, the less of it ‘melts’; therefore, the observed increase of ΔH_{exp} with $\Delta m\%$ is due to a decomposition requiring more enthalpy than melting, as it is generally the case. Among the ΔH_{d} values of Table 4, the differences are significant but small (less than 10%), while they are somehow larger for ΔH_{fus} . Note that

- F2 gives somehow higher ΔH_{d} values than F1, which is consistent with the role of F2 as the thermodynamically favored phase
- the presence of water vapor appears to slightly decrease ΔH_{d}
- ΔH_{fus} for F1 are ~20% higher than for F2
- a small decrease of ΔH_{fus} is associated with the presence of water vapor in both F1 and F2.

In summary, the above shows that forms F1 and F2 have very similar decomposition and melting behaviors. It is possible that some kind of exothermic reaction with water occurs upon melting, but its contribution appears to be independent of the scanning rate. Also, the decomposition mechanism is nearly insensitive to moisture in the measure cell.

A model for form F3

The fact that a different mechanism of decomposition and melting is active in form F3 is apparent from the results in dry atmosphere, where the peak enthalpy stays constant with increasing β (and $\Delta m\%$), as if the sublimation/evaporation processes causing the mass loss provided a negligible contribution to ΔH_{exp} . The substantial differ-

ence between experimental enthalpies in dry and wet nitrogen observed at low β (Table 3) decreases with increasing β , as if decomposition/melting was favored by a 'slow' reaction with water which has no time to complete at high scanning rates. If this is the case, it is appropriate to fit the enthalpy data of form F3 with the equation

$$\Delta H_{\text{exp}}^{\text{wN}} = \Delta H_{\text{exp}}^{\text{dN}} + A t_{\text{peak}} \quad (5)$$

where t_{peak} has been defined above and the superscripts refer to values measured in wet nitrogen (wN) and dry nitrogen (dN). By linear regression with enthalpy and t_{peak} data of form F3 in wet nitrogen we obtain (with a correlation of -0.99) an intercept of 156 J g^{-1} , well consistent with the directly determined average value $\Delta H_{\text{exp}}^{\text{dN}} \approx 154 \text{ J g}^{-1}$, and an enthalpy production rate for reaction with water $A \approx -5.5 \text{ J g}^{-1} \text{ min}^{-1}$. Of course, reaction with water is exothermic and its contribution is opposite to that of decomposition/melting.

Conclusions

The data of enthalpy and mass change as function of the scanning rate have been interpreted with a minimum set of very simple heuristic equations. Forms F1 and F2 in dry and wet nitrogen obey to Eq. (4), with nearly the same values for the 'apparent enthalpies' ΔH_{d} and ΔH_{fus} . The small but significant differences among fitting parameters point to the role of F2 as the most stable form of GV150526A, and to the role of water moisture as a co-adjuvant of decomposition and melting. On the other hand, form F3 follows Eq. (5), which hints to a different decomposition mechanism, where a slow reaction with water may play an important role. We recall that also structural evidence and dehydration behavior set F3 apart from the others. Therefore, this work completes a consistent phenomenological description of the thermal behavior of the three forms of GV150526A above room temperature.

References

- 1 A. Cugola, G. Gaviraghi and S. Giacobbe, Eur. Pat. Appl. EP 0 568 136 A1, 03 November 1993.
- 2 A. Marini, V. Berbenni, G. Bruni, C. Margheritis and A. Orlandi, J. Pharm. Sci., 90 (2001) 2131.